Electronic Supporting Information

Extending the Family of Tetrahedral Tectons: Phenyl Embraces in Supramolecular Polymers of Tetraphenylmethane-based Tetraphosphonic Acid Templated by Organic Bases

Jan K. Zaręba[*,†] Michał J. Białek[‡], Jan Janczak[§], Jerzy Zoń[*,⊥], and Agnieszka Dobosz[‖]

[†]Faculty of Chemistry, Wrocław University of Technology, 27 Wybrzeze Wyspianskiego Street, 50-370 Wrocław, Poland

[‡]Department of Chemistry, University of Wrocław, 14 F. Joliot-Curie Street, 50-383 Wrocław, Poland

[§]Institute of Low Temperature and Structural Research, Polish Academy of Sciences, 2 Okólna Street, P.O. Box 1410, 50-950 Wrocław, Poland

[⊥] Department of Thermodynamics, Machine and Thermal Device Theory, Faculty of Mechanical and Power Engineering, Wrocław University of Technology, 27 Wybrzeze Wyspianskiego Street, 50-370 Wrocław, Poland

[‖]Department of Basic Medical Sciences, Wrocław Medical University, 211 Borowska Street, 50-556 Wrocław, Poland

* (J.K.Z.) jan.zareba@pwr.edu.pl

* (J.Z.) jerzy.zon@pwr.edu.pl

Table of contents

Detailed synthetic procedures for phosphonic acids

All chemicals used in the synthesis were readily available from commercial sources (Sigma Aldrich, Merck, POCh) and were used as received. Infrared absorption spectra of solids were measured on a Perkin-Elmer FT-IR 1600 spectrophotometer in KBr discs. 1D and 2D NMR spectra for ^{1}H, ^{31}P and ^{13}C were recorded with Bruker Avance 500 or Bruker Avance III 600 instruments at the indicated frequencies and are referred to a residual solvent signal or H_3PO_4 standard. Phenyl signals (1-Ph, 2-Ph...) are assigned in respect to the location of a PO_3X_2 group. High resolution and accurate mass spectra were recorded using LCT Premier XE system with electrospray ionization and TOF analyzer. Melting points were determined using a Boetius apparatus and were uncorrected.

*Synthesis of tetrakis[4-(dihydroxyphosphoryl)phenyl]methane [**1**, TPPM]:*

Tetrakis[4-(dietoxyphosphoryl)phenyl]methane (1b)

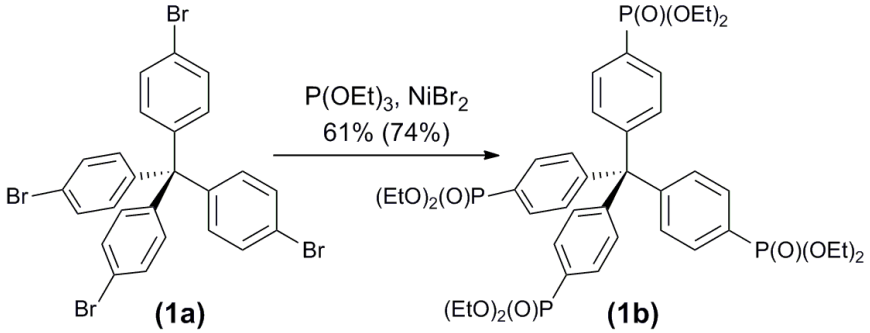

Tetra(4-bromophenyl)methane[1] (10.00 g, 15.7 mmol, **1a**) and *tert*-butylbenzene (25 cm^3, bp. 169 °C) were placed in a two-necked round-bottom flask equipped with condenser, gas inlet and bubbler, and heated to 170 °C under argon atmosphere. Next, anhydrous $NiBr_2$ (1.50 g, 6.86 mmol) was added and under continuous stirring, triethyl phosphite (15.0 cm^3, 87.5 mmol) was added dropwise over a period of 12 hours at the same temperature and under argon atmosphere. Usually, at this step, a reaction mixture contains mostly target compound **1a** and triphosphonylated monobromo derivative, according to TLC analysis (R_f = 0.09, a 10:1 (v/v) mixture of ethyl acetate : 96% ethanol as eluent, silica gel on PET foils with fluorescent indicator 254 nm, a UV lamp for the visualization). To complete phosphonylation, additional portion of anh. $NiBr_2$ (0.625 g, 2.86 mmol) was added and triethyl phosphite (7.5 cm^3, 43.7 mmol) was added dropwise over 8 hours under the same conditions as above. Then the reaction mixture was cooled and put into a refrigerator. Large amount of solid precipitated and was filtered while cold. This solid was dissolved in 100 cm^3 of ethyl acetate. Upon dissolution white precipitate has formed (probably some nickel complexes), which can be filtered. In order to remove residual nickel from crude product[2], 15% H_2O_2 (40 cm^3) was added, shaken and left overnight to extract nickel ions to water phase. The organic layer was separated, washed with water (40 cm^3), brine (40 cm^3) and dried over Na_2SO_4.

After filtration and evaporation of solvent, such an obtained slightly viscous light-orange solid was subjected to a crystallization procedure. The solid was dissolved in ethyl acetate (25 cm^3), and heated under reflux to obtain a clear solution. Then cyclohexane was added in small portions to achieve sustainable turbidity of the solution (about one third volume of ethyl acetate). Then the mixture was additionally refluxed for several minutes to obtain clear solution once again and, after gradual cooling, was put into a refrigerator overnight. Precipitated white solid was cold-filtered and washed with cyclohexane; crystallization can be repeated if necessary. Yield of **1b** from crystallization: 8.308 g (61%), mp. 173 – 182 °C.

Combined filtrates remained after crystallizations were evaporated and the residual solid was purified using column chromatography (R_f = 0.04, a 10:1 (v/v) mixture of ethyl acetate : 96% ethanol as eluent, silica gel on PET foils with fluorescent indicator 254 nm, a UV lamp for the visualization). Additional amount of **1b** from column chromatography: 1.770 g, mp. 177 – 184 °C.

Overall yield: 10.078 g (74%).

HRMS (ESI)**:** calcd for $C_{41}H_{57}O_{12}P_4$ ($M+H^+$): 865.2800; found: 865.2825 (*m/z*). **^{1}H NMR** (500 MHz, $CDCl_3$, 300 K) δ_H 7.68 (dd, $^3J_{P\text{-}H}$ = 12.9 Hz, $^3J_{H\text{-}H}$ = 8.4 Hz, 8H, 2-Ph), 7.27 (dd, $^3J_{H\text{-}H}$ = 8.4 Hz, $^5J_{P\text{-}H}$ = 3.8 Hz, 8H, 3-Ph), 4.19–4.04 (m, 16H, O-$\underline{CH_2}$-CH_3), 1.31 (t, $^3J_{H\text{-}H}$ = 7.1 Hz, 24H, O-CH_2-$\underline{CH_3}$) ppm. **^{31}P{^{1}H} NMR** (243 MHz, $CDCl_3$, 300 K): δ_P 18.76 (s) ppm. **^{13}C{^{1}H} NMR** (151 MHz, $CDCl_3$, 300 K) δ_C 149.35 (d, $^4J_{P\text{-}C}$ = 3.3 Hz, 4-Ph), 131.56 (d, $^2J_{P\text{-}C}$ = 10.0 Hz, 2-Ph), 130.88 (d, $^3J_{P\text{-}C}$ = 14.7 Hz, 3-Ph), 127.11 (d, $^1J_{P\text{-}C}$ = 191.2 Hz, 1-Ph), 65.67 (s, methane core), 62.45 (d, $^2J_{P\text{-}C}$ = 5.4 Hz, O-$\underline{CH_2}$-CH_3), 16.49 (d, $^3J_{P\text{-}C}$ = 5.6 Hz, O-CH_2-$\underline{CH_3}$) ppm. **IR** (KBr): ν_{max}, 3523 (m), 3422 (s), 2984 (m), 2933 (m), 2912 (m), 2871 (w), 1655 (w), 1599 (s), 1492 (m), 1481 (m), 1444 (m), 1395 (s), 1368 (m), 1235 (vs), 1163 (s), 1136 (s), 1098 (m), 1050 (vs), 1017 (vs), 973 (vs), 955 (vs), 824 (m), 793 (s), 766 (s), 728 (m), 712 (s), 699 (m), 635 (m), 578 (s), 540 (s) cm^{-1}.

Tetrakis[4-(dihydroxyphosphoryl)phenyl]methane (1)

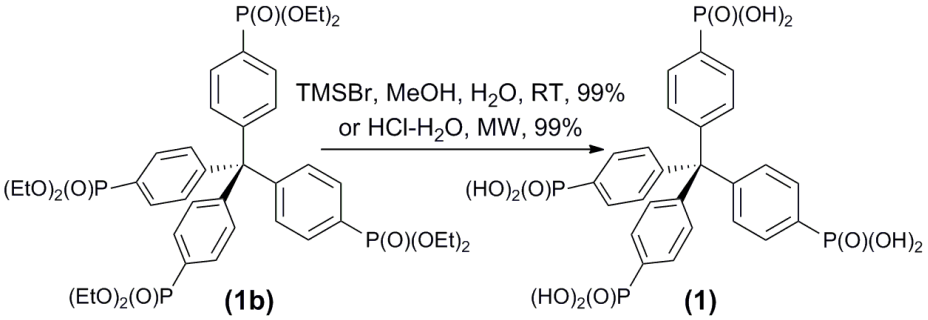

Method *via trans*-silylation

Tetrakis[4-(dietoxyphosphoryl)phenyl]methane (2.268 g, 2.62 mmol, **1b**), was dissolved in dichloromethane (15 cm^3) and trimethylsillyl bromide (TMSBr) (4.2 cm^3, 31.84 mmol) was added dropwise. An obtained mixture was stirred for 16 hours at 25 °C. Then the mixture was evaporated under reduced pressure. To the resulting beige solid methanol (40 cm^3) was added and evaporated three times.

An obtained product can be additionally purified by refluxing octasodium salt with active carbon powder in water and subsequent precipitation of acid **1** by acidification with 36% hydrochloric acid.

Pure acid **1** was obtained as an off-white solid: 1.680 g (99%), mp. > 360 °C.

Microwave method

Tetrakis[4-(dietoxyphosphoryl)phenyl]methane (1.000 g, 2.62 mmol, **1b**), was dispersed in a 1:1 mixture of water and concentrated hydrochloric acid (20 cm^3), transferred to 50 mL microwave Teflon vessel, and tightly closed. An obtained mixture was heated at 170 °C for 2 hours at 30% of the maximum power in a high-pressure solvothermal microwave reactor ERTEC Magnum II.

Pure acid **1** was obtained as an off-white solid: 0.730 g (99%), mp. > 360 °C.

HRMS (ESI)**:** calcd for $C_{25}H_{23}O_{12}P_4$ ($M-H^-$): 639.0140; found: 639.0142 (*m/z*). **^{1}H NMR** (600 MHz, DMSO-d_6, 300 K) δ_H 7.63 (dd, $^3J_{P\text{-}H}$ = 12.5 Hz, $^3J_{H\text{-}H}$ = 8.4 Hz, 8H, 2-Ph), 7.33 (dd, $^3J_{H\text{-}H}$ = 8.5 Hz, $^5J_{P\text{-}H}$ = 3.0 Hz, 8H, 3-Ph), 3.87 (br s, 8H, P-$\underline{OH}$) ppm. **^{31}P{^{1}H} NMR** (202 MHz, DMSO-d_6, 300 K): δ_P 13.14 (s) ppm. **^{13}C{^{1}H} NMR** (126 MHz, DMSO-d_6, 300 K) δ_C 148.31 (d, $^4J_{P\text{-}C}$ = 3.2 Hz, 4-Ph), 131.86 (d, $^1J_{P\text{-}C}$ = 181.9 Hz, 1-Ph), 130.49 (d, $^2J_{P\text{-}C}$ = 10.2 Hz, 2-Ph), 129.91 (d, $^3J_{P\text{-}C}$ = 14.2 Hz, 3-Ph), 64.97 (s, methane core) ppm.

IR (KBr): ν_{max}, 3420 (br m), 3034 (s), 2853 (br s), 2277 (br s), 1602 (s), 1501 (m), 1404 (m), 1207 (vs), 1189 (vs), 1147 (vs), 1044 (vs), 1017 (vs), 939 (vs), 912 (s), 845 (m), 818 (s), 752 (m), 734 (m), 711 (s), 700 (s), 559 (s), 533 (vs), 480 (s) cm^{-1}.

The synthesis of acid-base adducts

Adduct of TPPM and pyridine, (2)

TPPM (0.015 g, 0.0234 mmol) was mixed with distilled water (2.0 cm^3) and excess of pyridine (about 0.2 cm^3, 2.48 mmol). Obtained solution was left undisturbed for slow evaporation at room temperature conditions. After a few days, obtained precipitate was solved in additional amount of water and left for slow evaporation. After another few days rectangular, colorless crystals of **2** appeared. Yield: 15.0 mg (85%), **IR** (KBr) ν_{max}, 3435 (m), 3383 (w), 3335 (w), 3177 (w), 3135 (w), 3096 (w), 3070 (w), 3029 (w), 2852(w), 2803 (w), 2752 (m), 2286 (m), 2157 (w), 1940 (w), 1634 (m), 1598 (s), 1551 (w), 1487 (s), 1398 (m), 1138 (s), 1036 (m), 983 (s), 931 (s), 908 (s), 819 (s), 753 (m), 708 (s), 635 (w), 606 (w), 564 (w), 532 ()m, 446 (w) cm^{-1}

Adduct of TPPM and 2,2'-bipyridine, (3)

TPPM (0.0175 g, 0.0273 mmol) and 2,2'-bipyridine (0.0172 g, 0.110 mmol) were mixed with distilled water (3.0 cm^3) and heated under reflux for a few minutes. Dioxane (0.6 cm^3) was added to the resulting mixture and heated again under reflux for a few minutes. After addition of dioxane, solution turns light purple (earlier was colorless). Obtained solution was left undisturbed for evaporation at room temperature conditions. After several days small, colorless needle crystals of **3** appeared, amongst significant amount of crystallized 2,2'-bipyridine.

Yield: 8.8 mg (34%), **IR** (KBr) ν_{max}, 3430 (w), 3095 (w), 3065 (w), 3034 (w), 2694 (m), 2224 (m), 1598 (m), 1564 (m), 1496 (w), 1472 (w), 1429 (m), 1399 (w), 1279 (w), 1261 (m), 1215 (s), 1201 (s), 1168 (m), 1135 (s), 1039 (m), 989 (s), 970 (s), 936 (s), 907 (s), 819 (s), 760 (s), 745 (m), 707 (s), 649 (m), 574 (m), 539 (vs), 463 (s) cm^{-1}.

Adduct of TPPM and 4-(*N*,*N*-dimethylamino)pyridine, (4)

TPPM (0.0247 g, 0.0385 mmol) and 4-(*N,N*-dimethylamino)pyridine (0.0144 g, 0.118 mmol) were mixed with distilled water (4.0 cm^3) and heated under reflux for a few minutes. Dimethylacetamide (DMA) (1.0 cm^3) was added to the resulting mixture and it was heated again under reflux for a few minutes. Small amount of undissolved residue was filtrated. Obtained solution was left undisturbed for evaporation at room temperature conditions. After several days big twinned, colorless plate crystals of **4** appeared. Yield: 18.2 mg (43%), **IR** (KBr) ν_{max}, 3396 (s), 3240 (m), 3078 (s), 3064 (s), 2940 (s), 2775 (s), 2678 (s), 2342 (m), 2061 (m), 1959 (m), 1648 (vs), 1599 (s), 1560 (vs), 1493 (m), 1444 (s), 1399 (s), 1220 (s), 1137 (vs), 1060 (s), 1044 (s), 1018 (s), 932 (s), 902 (s), 818 (vs), 743 (s), 706 (s), 635 (m), 568 (s), 538 (vs) cm^{-1}.

Adduct of TPPM and 1,6-diaminohexane, (5) and (5B)

TPPM (0.0200 g, 0.0312 mmol) and 1,6-diaminohexane (0.0109 g, 0.0777 mmol) were mixed with distilled water (3.0 cm^3) and heated under reflux for a few minutes. DMSO (1.0 cm^3) and methanol (0.5 cm^3) were added to the resulting mixture and it was heated again under reflux for a few minutes. Undissolved residue was filtrated. After partial solvent evaporation (about a month at room temperature conditions), colorless single crystals appeared. Among them **5** and **5b** were selected. Yield: 14.7 mg, **IR** (KBr) ν_{max}, 3393 (s), 3189 (s), 3027 (s), 2934 (s), 2863 (s), 2658 (s), 2471 (m), 2359 (m), 2150 (m), 1638 (s), 1598 (s), 1526 (m), 1494 (m), 1474 (m), 1397 (m), 1252 (m), 1237 (m), 1138

(vs), 1044 (vs), 1017 (s), 951 (s), 929 (s), 898 (s), 819 (s), 791 (m), 740 (m), 706 (s), 636 (m), 576 (s), 544 (vs), 492 (s), 478 (s) cm^{-1}.

Adduct of TPPM and urotropine, (6)

TPPM (0.0200 g, 0.0312 mmol) and urotropine (0.0109 g, 0.0777 mmol) were mixed with distilled water (3.0 cm^3) and heated under reflux for a few minutes. To the resulting mixture DMSO (1.0 cm^3) and methanol (0.5 cm^3) were added and heated again under reflux for a few minutes. Undissolved residue was filtrated. After partial solvent evaporation (about a month at room temperature conditions), colorless single crystals of **6** appeared. Yield: 22.8 mg (60%), **IR** (KBr) ν_{max}, 3424 (s), 3199 (s), 3011 (s), 2938 (s), 2901 (s), 2822 (s), 2689 (s), 2568 (s), 2482 (s), 2404 (s), 2347 (s), 1674 (m), 1645 (m), 1600 (m), 1465 (s), 1437 (s), 1403 (s), 1368 (m), 1312 (m), 1261 (s), 1221 (s), 1140 (vs), 1076 (s), 1062 (s), 1031 (vs), 1016 (vs), 983 (vs), 955 (s), 925 (s), 901 (s), 824 (s), 794 (s), 753 (m), 736 (m), 712 (s), 694 (s), 659 (s), 635 (m), 577 (s), 541 (vs), 500 (s), 485 (s), 468 (s) cm^{-1}.

Supplementary tables

Table S1. Selected distances [Å] and angles [°] for all structures

*Adduct of TPPM and pyridine (**2**)*					
P1-O4	1.5438(18)	**P1-C11**	1.790(2)	**P2-O3**	1.5070(18)
P1-O5	1.5482(15)	**P2-O1**	1.5201(16)	**P2-C5**	1.8013(19)
P1-O6	1.4985(17)	**P2-O2**	1.5580(18)	**C14-N1-C16**	119.3(3)
*Adduct of TPPM and 2,2'-bipyridine (**3**)*					
P1-O1	1.471(3)	**P1-O3**	1.547(3)	**C8-N1-C9**	118.2(3)
P1-O2	1.534(3)	**P1-C5**	1.788(4)		
*Adduct of TPPM and 4-(N,N-dimethylamino)pyridine (**4**)*					
P11-O11	1.495(3)	**P21-C24**	1.796(4)	**P41-O42**	1.502(3)
P11-O12	1.499(3)	**P31-O31**	1.495(3)	**P41-O43**	1.575(3)
P11-O13	1.552(3)	**P31-O32**	1.515(3)	**P41-C44**	1.793(4)
P11-C14	1.789(4)	**P31-O33**	1.539(3)	**C62-N61-C66**	120.6(5)
P21-O21	1.490(3)	**P31-C34**	1.790(4)	**C72-N71-C76**	120.3(5)
P21-O22	1.488(3)	**P41-O41**	1.469(3)	**C52-N51-C56**	120.1(5)
P21-O23	1.561(3)				
*Adduct of TPPM and 1,6-hexyldiamine (**5**)*					
P11-O11	1.473(3)	**P21-C24**	1.784(4)	**P41-O43**	1.540(4)
P11-O12	1.512(3)	**P31-O31**	1.495(3)	**P41-C44**	1.780(5)
P11-O13	1.550(2)	**P31-O32**	1.505(3)	**N51-C52**	1.486(6)
P11-C14	1.771(4)	**P31-O33**	1.540(4)	**N58-C57**	1.467(6)
P21-O21	1.488(3)	**P31-C34**	1.799(4)	**N61-C62**	1.454(7)
P21-O22	1.485(3)	**P41-O41**	1.446(4)	**N71-C72**	1.446(4)
P21-O23	1.577(3)	**P41-O42**	1.547(5)		
*Adduct of TPPM and urotropine (**6**)*					
P1-O11	1.493(2)	**P2-O21**	1.498(3)	**C3-N1-C4**	108.1(3)
P1-O12	1.507(3)	**P2-O22**	1.502(2)	**C2-N1-C3**	109.2(2)
P1-O13	1.569(2)	**P2-O23**	1.566(3)	**C2-N1-C4**	107.9(2)
P1-C14	1.813(3)	**P2-C24**	1.809(3)	**C5-N4-C7**	109.0(3)
C5-N2-C6	109.0(4)	**C3-N3-C6**	107.8(4)	**C4-N4-C5**	109.0(4)
C2-N2-C6	109.5(3)	**C6-N3-C7**	107.8(3)	**C4-N4-C7**	108.0(4)
C2-N2-C5	109.3(3)	**C3-N3-C7**	108.9(3)		
*2nd adduct of TPPM and 1,6-hexyldiamine (**5b**)*					
Disordered group **P11** **A:** 0.696 **B:** 0.304		Disordered group **P31** **A:** 0.685 **B:** 0.315		**P21-O21**	1.475(3)
A: P11-O11	1.443(4)	**A: P31-O31**	1.468(4)	**P21-O22**	1.514(3)
B: P11-O14	1.440(8)	**B: P31-O34**	1.465(8)	**P21-O23**	1.602(3)
A: P11-O12	1.512(3)	**A: P31-O32**	1.525(5)	**P21-C24**	1.795(3)
B: P11-O15	1.527(8)	**B: P31-O35**	1.502(12)	**P41-O41**	1.492(3)
A: P11-O13	1.622(5)	**A: P31-O33**	1.573(5)	**P41-O42**	1.499(3)
B: P11-O16	1.582(7)	**B: P31-O36**	1.580(16)	**P41-O43**	1.558(3)
P1-C14	1.799(3)	**P31-C34**	1.811(3)	**P41-C44**	1.794(3)
N51-C52	1.464(5)	**N58-C57**	1.480(5)		
N71-C72	1.473(8)	**N61-C62**	1.453(5)		

Table S2. Potential hydrogen bonds in all structures, determined from geometrical criteria ($d_{D\cdots A}$ < $R_D + R_A + 0.50$, $d_{H\cdots A} < R_H + R_A - 0.12$, Ang.$_{D\text{-}H\cdots A} > 100.0^o$)

D-H···A	D-H [Å]	H···A [Å]	D···A [Å]	D-H···A
*Adduct of TPPM and pyridine (**2**)*				
N1-H1N···O3$^{(i)}$	0.8700	2.1000	2.906(3)	154
O1-H1O···O1$^{(i)}$	1.2300	1.2300	2.469(3)	180
O1W-H1W···O1$^{(i)}$	0.92(4)	1.99(3)	2.893(3)	166(3)
O2-H2O···O1W$^{(ii)}$	0.86(3)	1.76(3)	2.615(3)	172(3)
O1W-H2W···O6$^{(iii)}$	0.82(4)	2.11(4)	2.921(3)	171(3)
O4-H4O···O3$^{(iv)}$	1.03(3)	1.48(3)	2.490(2)	167(3)
O5-H5O···O6$^{(v)}$	0.89(3)	1.70(3)	2.578(2)	174(2)
C13-H13···O2$^{(vi)}$	0.9300	2.5100	3.245(3)	136.00
C14-H14···O4$^{(vii)}$	0.9300	2.5200	3.251(4)	135.00
(i) 1-x,2-y,1-z; (ii) 1-x,1-y,1-z; (iii) 1-x,1+y,1/2-z; (iv) 3/2-x,1/2-y,1-z; (v) 3/2-x,-1/2+y,1/2-z; (vi) x,1-y,-1/2+z; (vii) -1/2+x,1/2+y,z				
*Adduct of TPPM and 2,2'-bipyridine (**3**)*				
O2-H1O···N1$^{(i)}$	0.77(5)	1.88(5)	2.632(4)	169(6)
O3-H2O···O1$^{(ii)}$	0.90(5)	1.68(6)	2.551(4)	159(5)
C12-H12···O2$^{(iii)}$	0.9300	2.5000	3.312(5)	146.00
(i) -x,1-y,z; (ii) 1/2-x,3/2-y,-1/2+z; (iii) -1+y,1-x,-z				
*Adduct of TPPM and 4-(N,N-dimethylamino)pyridine (**4**)*				
O13-H13O···O12$^{(i)}$	0.8200	1.8400	2.586(4)	151.00
O23-H23O···O11$^{(ii)}$	0.8200	1.8500	2.627(4)	157.00
O33-H33O···O22$^{(iii)}$	0.8200	1.7500	2.507(4)	152.00
O42-H42O···O42$^{(iv)}$	1.2200	1.2200	2.446(4)	180.00
O43-H43O···O31$^{(v)}$	0.8200	1.8100	2.611(4)	164.00
N51-H51···O11$^{(v)}$	0.8600	1.8400	2.682(5)	166.00
N61-H61···O21	0.8600	1.7700	2.623(5)	173.00
O1W-H1W1···O2W$^{(vi)}$	0.8300	2.0200	2.767(6)	150.00
O1W-H2W1···O32$^{(vi)}$	0.8300	2.4400	3.187(6)	150.00
O2W-H1W2···O12$^{(vii)}$	0.8100	1.9700	2.764(4)	167.00
O2W-H2W2···O41$^{(viii)}$	0.8300	1.9800	2.806(5)	175.00
O3W-H1W3···O41$^{(ix)}$	0.8200	1.9900	2.799(5)	169.00
O3W-H2W3···O13	0.8300	2.1400	2.899(5)	152.00
O4W-H1W4···O32	0.8200	1.8000	2.584(4)	160.00
O4W-H2W4···O6W	0.8200	1.7700	2.589(8)	180.00
O5W-H1W5···O41$^{(viii)}$	0.8200	2.1800	2.989(5)	167.00
O6W-H1W6···O21$^{(iii)}$	0.8100	1.9400	2.748(5)	175.00
C33-H33···O1W$^{(vii)}$	0.9300	2.4400	3.339(6)	164.00
C45-H45···O42	0.9300	2.5300	2.924(5)	106.00
C56-H56···O22$^{(iii)}$	0.9300	2.3700	3.123(6)	138.00
C66-H66···O3W$^{(iii)}$	0.9300	2.3400	3.062(7)	134.00
(i) 1/2-x,3/2-y,1-z; (ii) x,1-y,-1/2+z; (iii) 1/2-x,-1/2+y,1/2-z; (iv) 1-x,-y,1-z; (v) 1/2-x,1/2-y,1-z; (vi) x,1-y,1/2+z; (vii) x,1-y,-1/2+z; (viii) 1/2-x,1/2+y,1/2-z; (ix) 1/2-x,3/2-y,1-z;				

*Adduct of TPPM and 1,6-hexyldiamine (**5**)*				
O13-H13O···O21[(i)]	0.815(19)	1.75(2)	2.545(3)	164(2)
O23-H23O···O12[(ii)]	0.820(13)	1.762(12)	2.561(4)	164.5(18)
O33-H33O···O31[(iii)]	0.820(9)	1.758(8)	2.564(4)	167(2)
O42-H42O···O3W[(iv)]	0.819(12)	1.904(9)	2.635(8)	148.0(9)
O43-H43O···O32[(v)]	0.820(14)	1.880(12)	2.619(4)	149.3(10)
N51-H511···O1W[(vi)]	0.85(4)	2.05(4)	2.835(6)	154(4)
N51-H513···O23[(vii)]	0.85(2)	2.19(2)	2.985(5)	156(4)
N58-H582···O12[(vii)]	0.85(4)	2.01(4)	2.748(4)	145(4)
N71-H711···O4W	0.890(5)	2.066(6)	2.951(5)	172.7(5)
N71-H712···O2W	0.891(6)	2.130(5)	2.933(4)	149.6(5)
Potential hydrogen bonds (not localized hydrogen atoms)				
O41···O5W	-	-	2.95(1)	-
O41···O1W	-	-	2.933(5)	-
O1W···O11	-	-	2.738(4)	-
O4W···O41	-	-	2.760(5)	-
O41···O2W	-	-	2.800(4)	-
O5W···O11	-	-	3.11(1)	-
O21···O2W	-	-	2.734(5)	-
O43···O5W	-	-	3.07(1)	-
O32···N61	-	-	2.745(5)	-
O22···N61	-	-	2.779(6)	-
N61···O3W	-	-	3.126(7)	-
N58···O31	-	-	2.804(3)	-
O43···N58	-	-	2.944(6)	-
O5W···N58	-	-	2.83(1)	-
N51···O13	-	-	3.078(5)	-
O13···N51	-	-	3.171(6)	-
N51···O22	-	-	2.856(4)	-
N71···O11	-	-	2.758(3)	-
N71···O1W	-	-	3.140(3)	-

(i) x,-1+y,z; (ii) 2-x,1-y,1-z; (iii) -x,1-y,2-z; (iv) 1-x,-y,2-z; (v) 1+x,y,z; (vi) -1+x,1+y,z; (vii) -1+x,y,z

*Adduct of TPPM and urotropine (**6**)*				
N1-H1 ···O12[(i)]	0.8700	1.8700	2.727(4)	167.00
N3-H3 ···O3W (occ. 0.5)	0.8700	2.4800	3.295(7)	157.00
N3-H3 ···O4W (occ. 0.5)	0.8700	2.5300	3.382(10)	167.00
O13-H13O···O21[(ii)]	0.8200	1.8000	2.557(3)	152.00
O23-H23O···O22[(iii)]	0.8200	1.8200	2.623(3)	165.00
C2-H2A···O1W[(iv)]	0.9700	2.5200	3.458(4)	163.00
C2-H2B···O1[(i)]	0.9700	2.5600	3.481(5)	158.00
C3-H3B···O21[(v)]	0.9700	2.3500	3.321(4)	175.00
C23-H23···O13[(vi)]	0.9300	2.4800	3.381(3)	164.00

(i) x,-y,-1/2+z; (ii) x,-y,-1/2+z; (iii) -x,1-y,1-z; (iv) 1/2-x,1/2-y,1-z; (v) x,1-y,-1/2+z; (vi) 1/2-x,1/2+y,1/2-z;

NMR Spectra and discussion

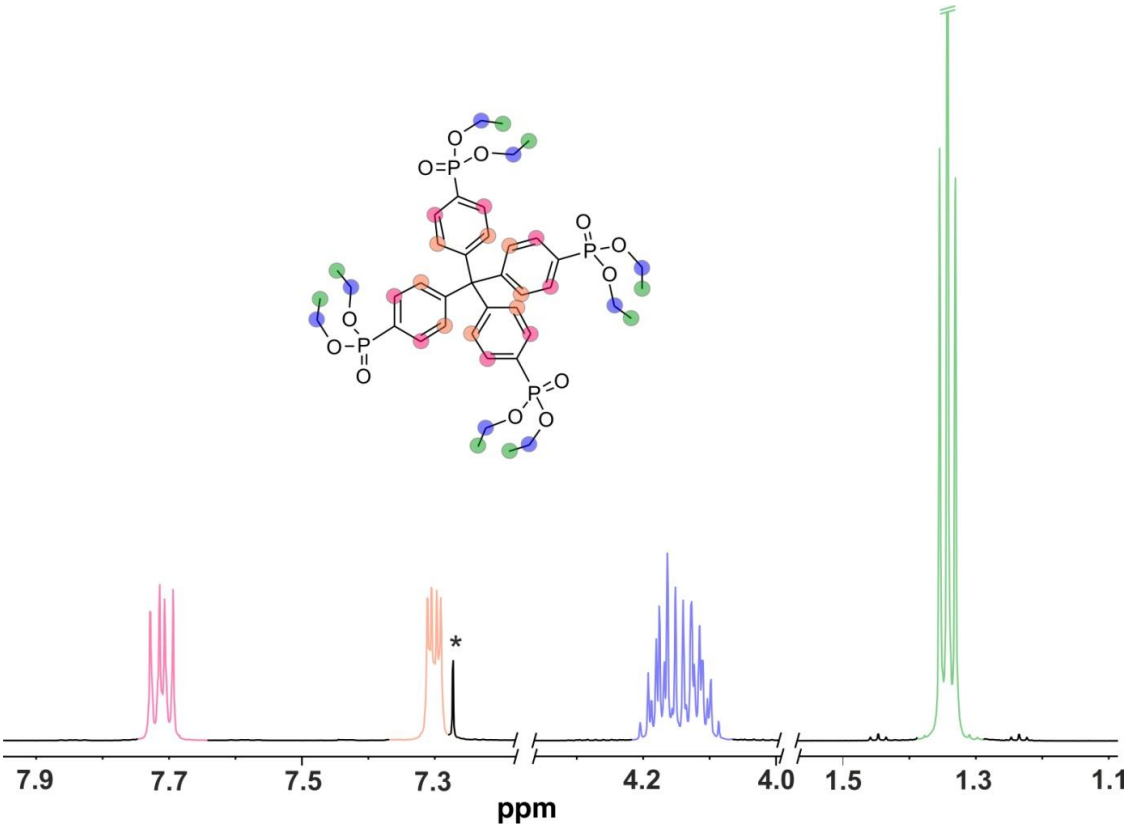

Figure S1. A ^{1}H NMR spectrum (600MHz, $CDCl_3$, 300 K) of ester **1b**.

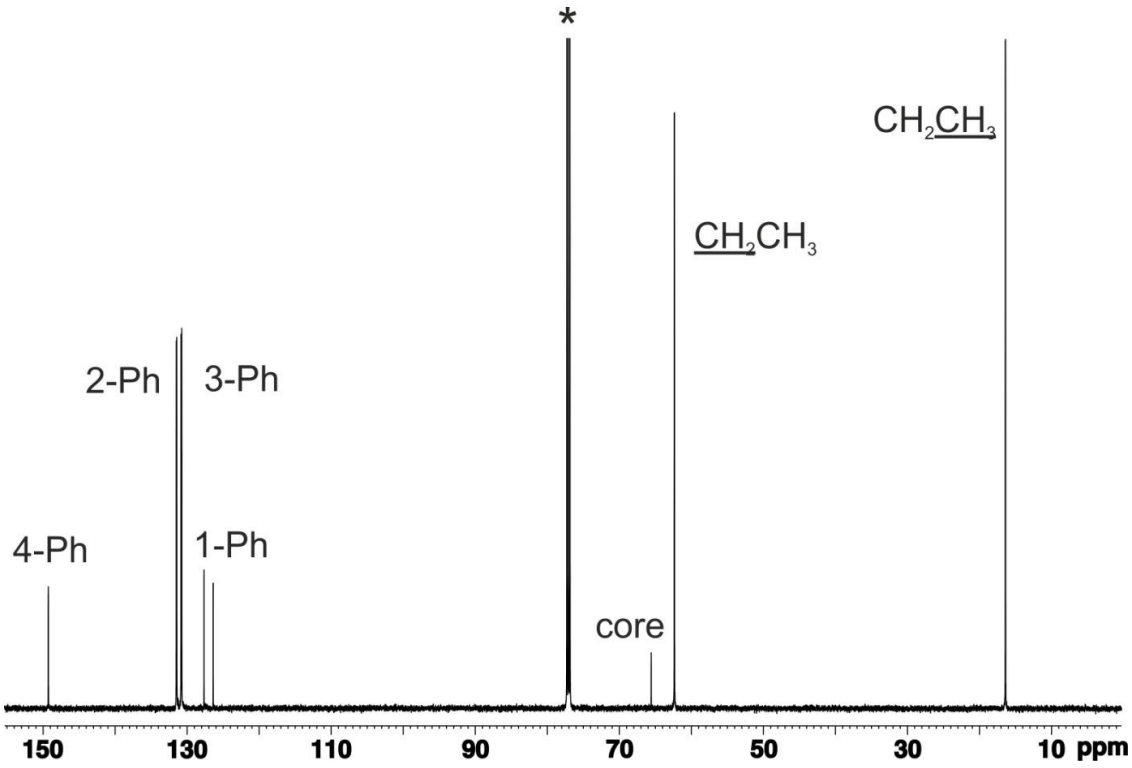

Figure S2. A ^{13}C NMR spectrum (151 MHz, $CDCl_3$, 300 K) of ester **1b**.

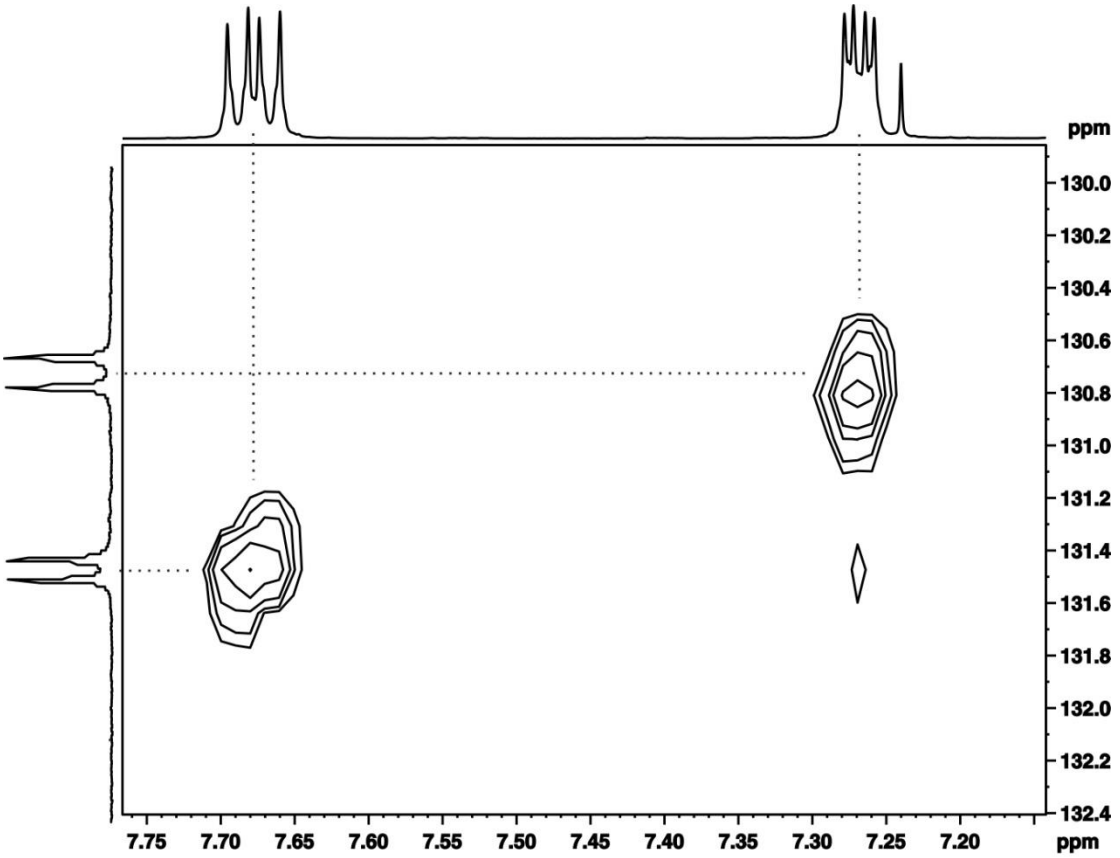

Figure S3. A fragment of **1b** HSQC spectrum showing correlations (cross-peaks and dotted lines) between phenyl protons and corresponding carbon atoms' signals.

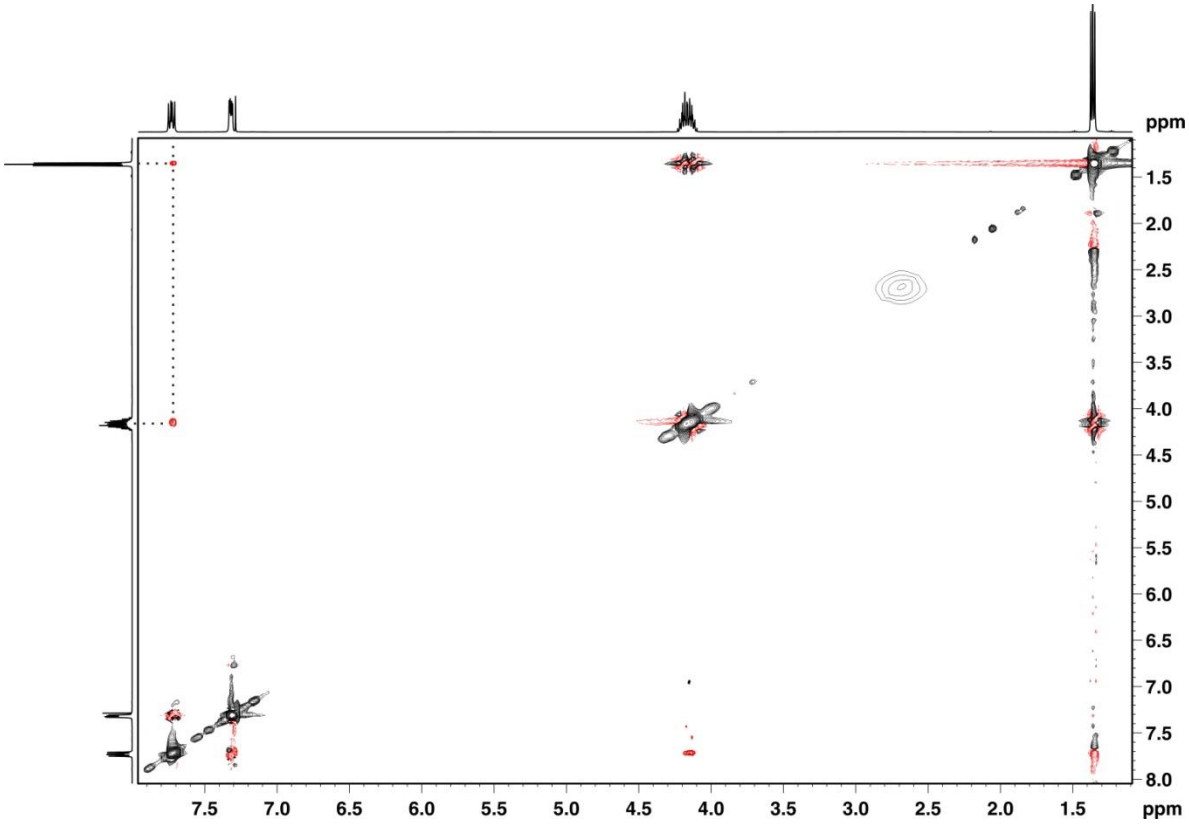

Figure S4. A NOESY spectrum of ester **1b** showing correlations through space (red cross-peaks and dotted lines) between 2-Ph phenyl protons and alkyl chain from the phosphonic group.

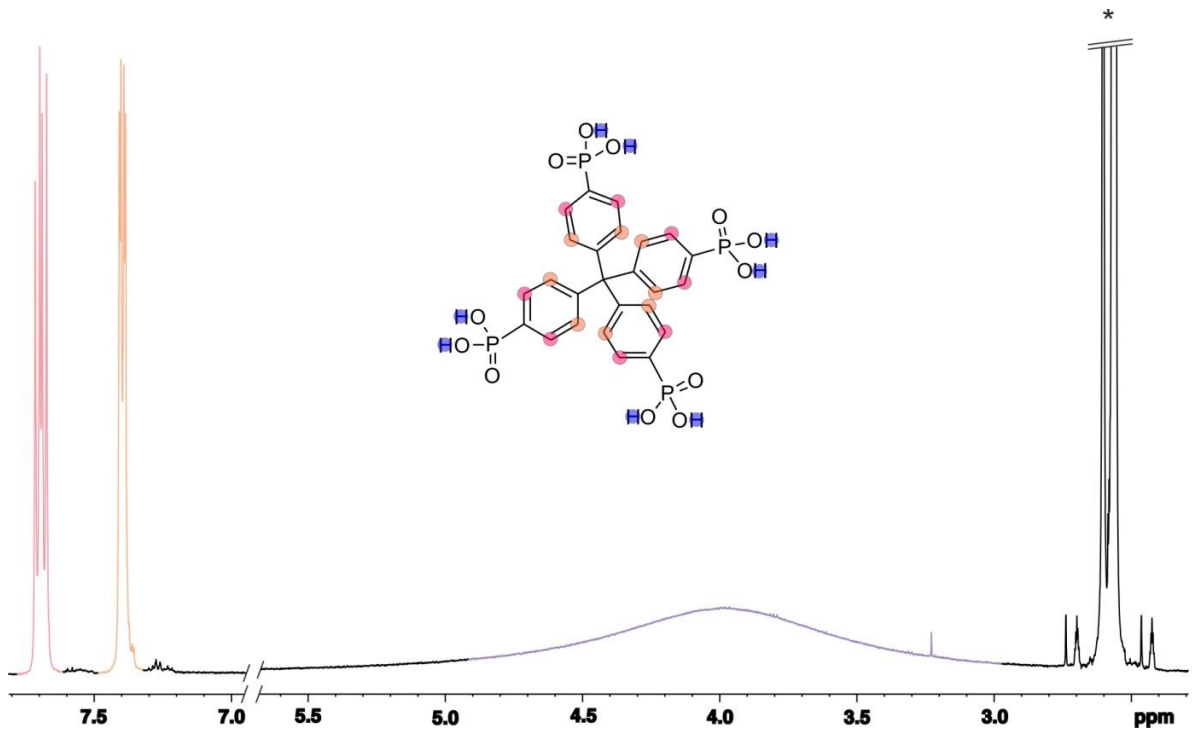

Figure S5. A ^{1}H NMR spectrum (500 MHz, DMSO-d_6, 300 K) of TPPM (**1**).

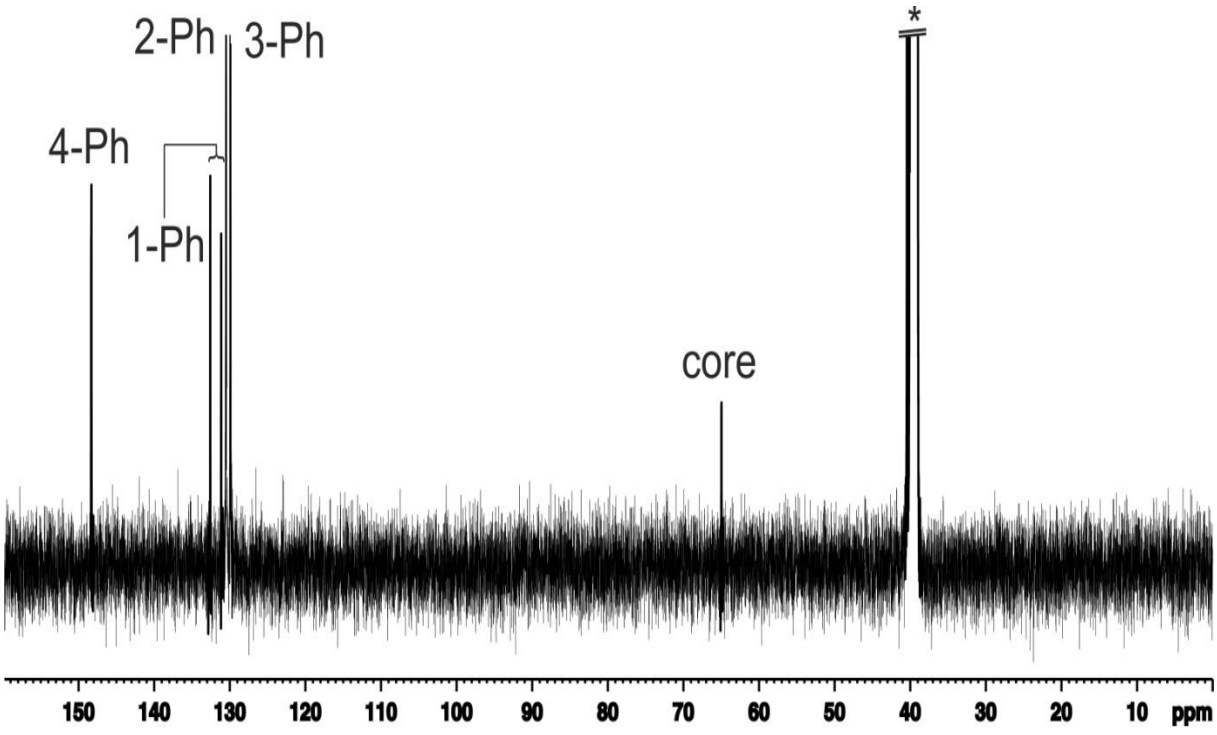

Figure S6. A ^{13}C NMR spectrum (126 MHz, DMSO-d_6, 300 K) of TPPM (**1**).

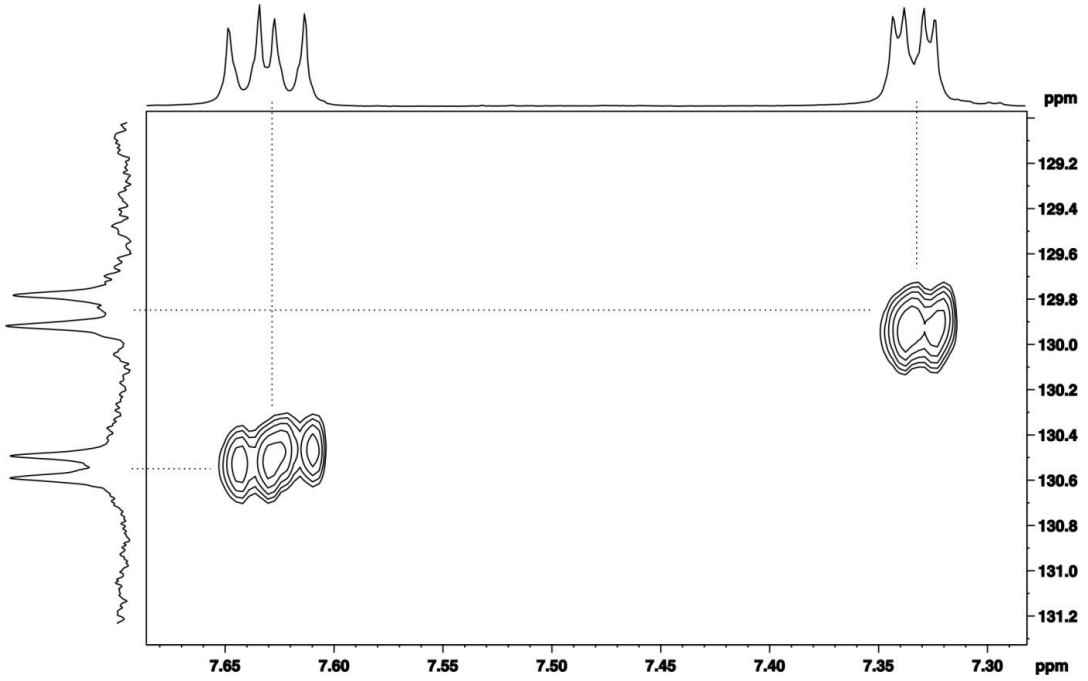

Figure S7. A fragment of a TPPM (**1**) HSQC spectrum showing correlations (cross-peaks and dotted lines) between phenyl protons and corresponding carbon atoms' signals analogically to the ester spectrum.

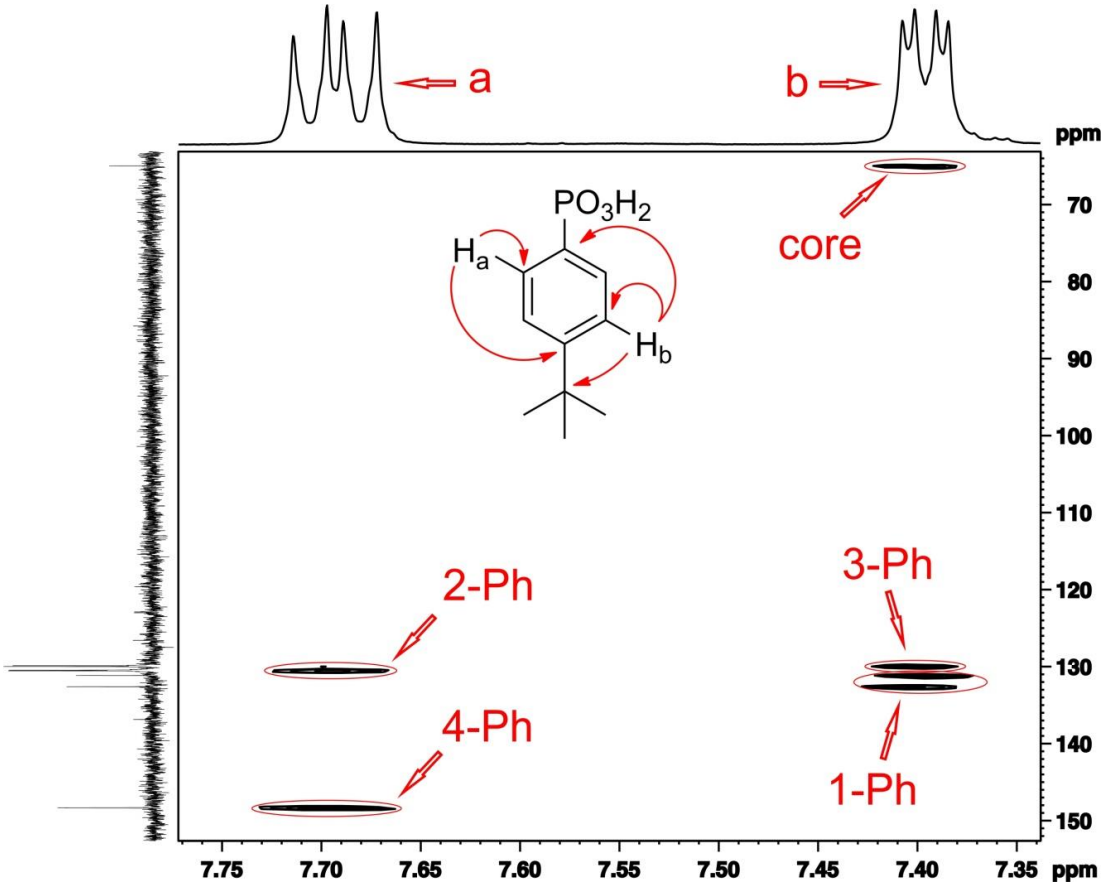

Figure S8. A TPPM (**1**) HMBC spectrum showing correlations (cross-peaks): for signal a (2-Ph), there are correlations through one and three bonds, also weaker through two bonds to 3-Ph and 1-Ph (not shown). Signal b (3-Ph) correlates through one and three bonds and weakly through two bonds to 2-Ph (not shown).

Supplementary Figures

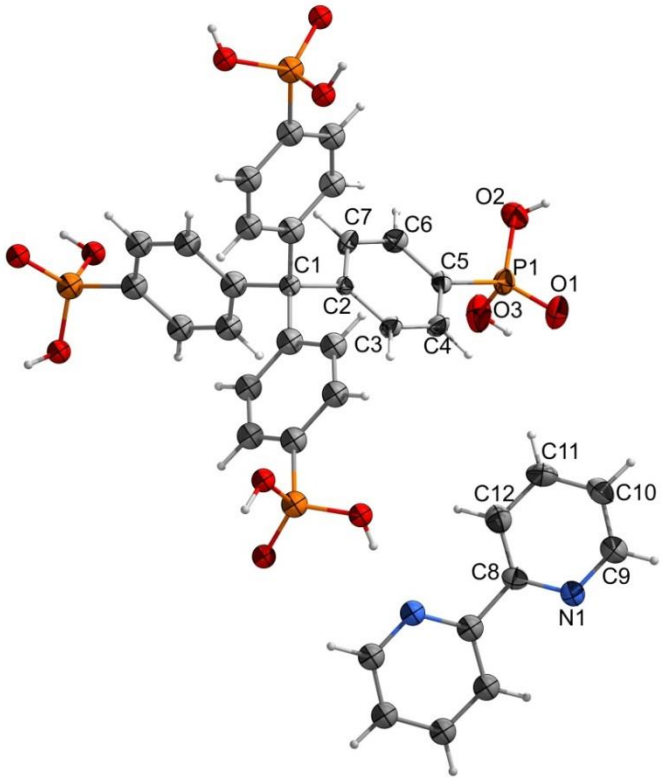

Figure S9. The asymmetric unit of adduct **3** (only atoms with labels). Displacement ellipsoids are drawn at the 50% probability level. Hydrogen atoms drawn arbitrarily small.

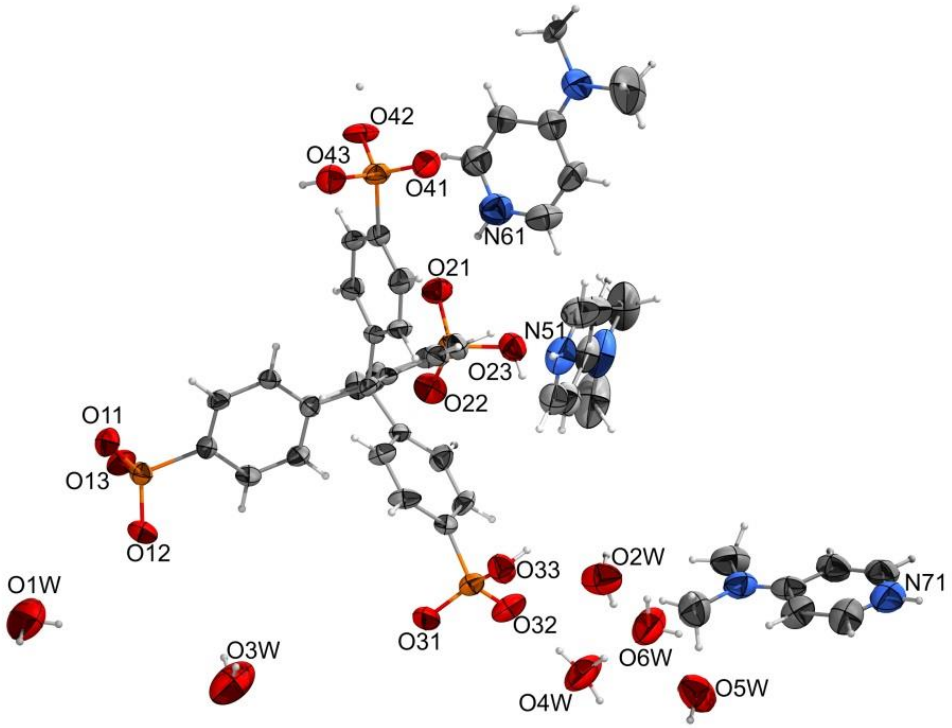

Figure S10. The asymmetric unit of adduct **4**. Displacement ellipsoids are drawn at the 50% probability level. Hydrogen atoms drawn arbitrarily small.

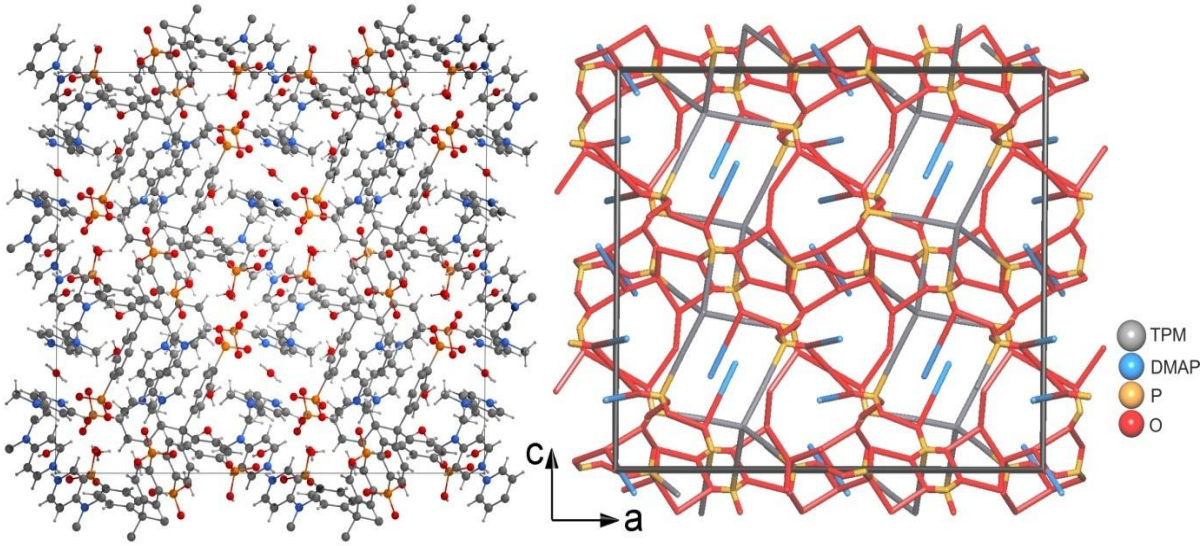

Figure S11. A packing diagram of adduct **4** (left) together with partial topological simplification (right) showing high complexity of the obtained network.

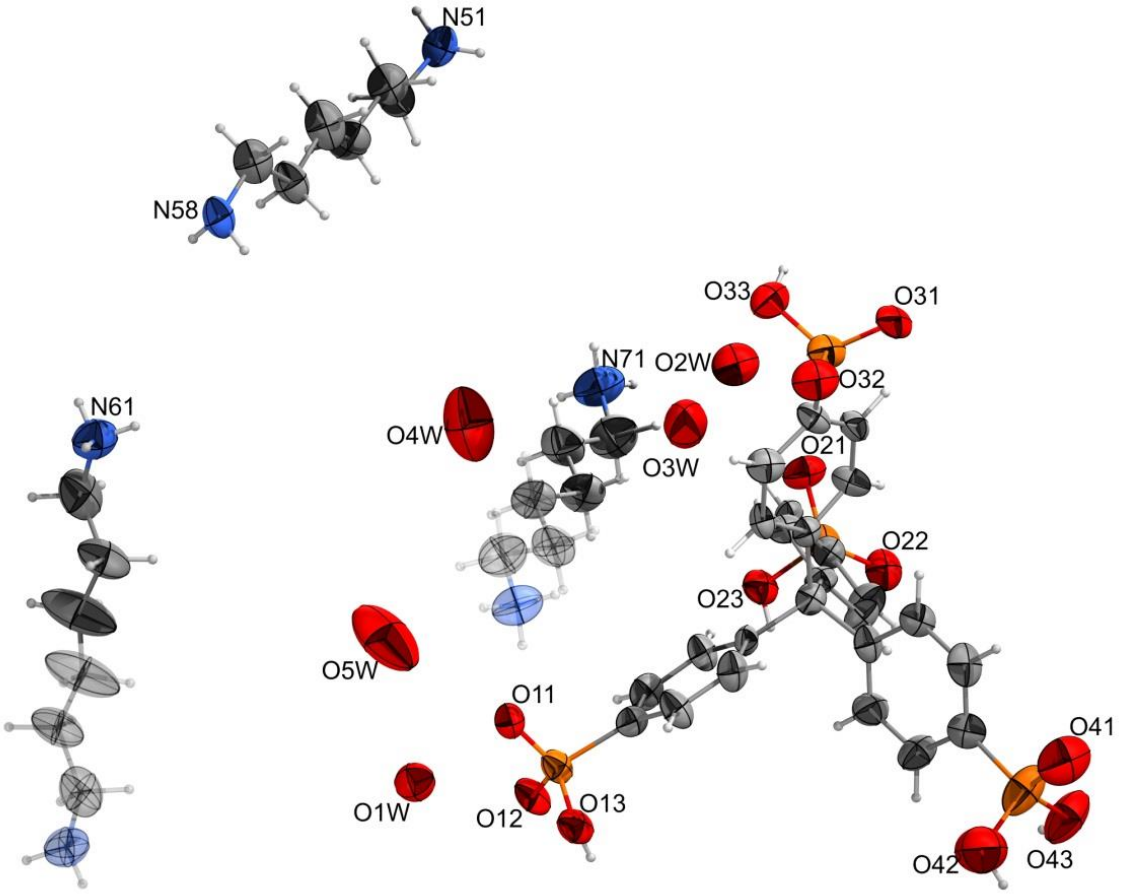

Figure S12. The asymmetric unit of adduct **5** (only non-transparent atoms). Displacement ellipsoids are drawn at the 50% probability level. Hydrogen atoms drawn arbitrarily small.

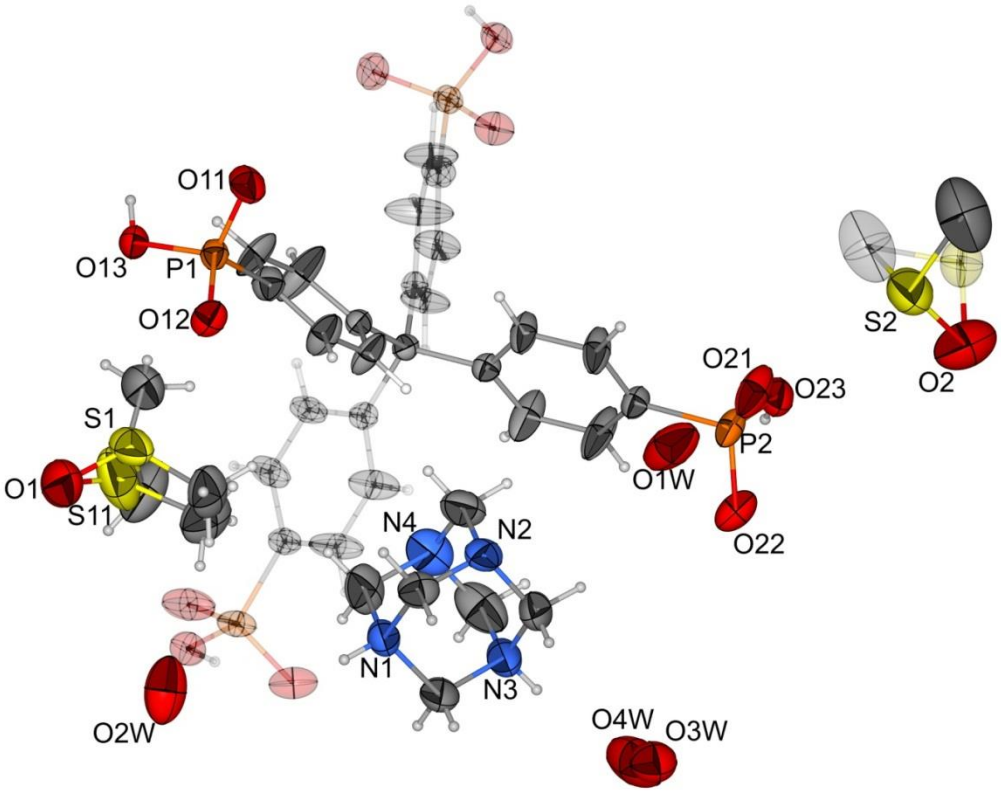

Figure S13. The asymmetric unit of adduct **6** (only non-transparent atoms). Displacement ellipsoids are drawn at the 50% probability level. Hydrogen atoms drawn arbitrarily small.

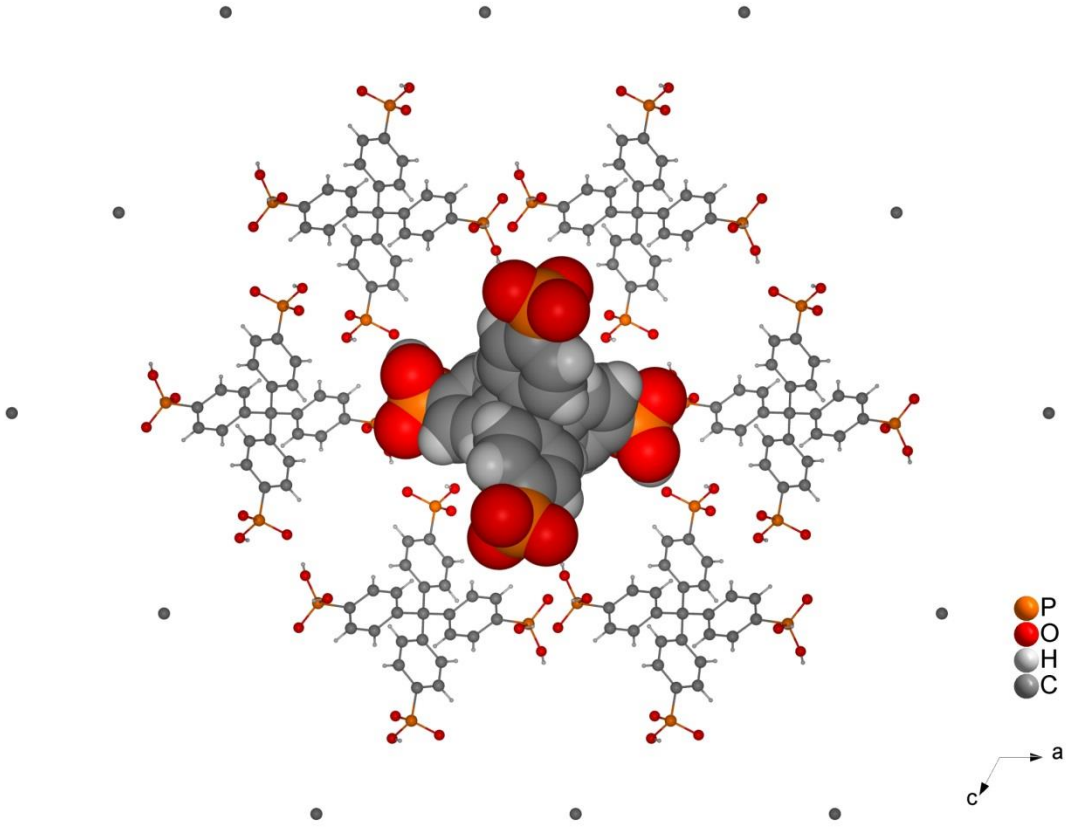

Figure S14. A pseudohexagonal arrangement of 4PE-held linear columns in adduct **2** crystal. Grey isolated atoms are quaternary carbon ones from TPPM molecules.

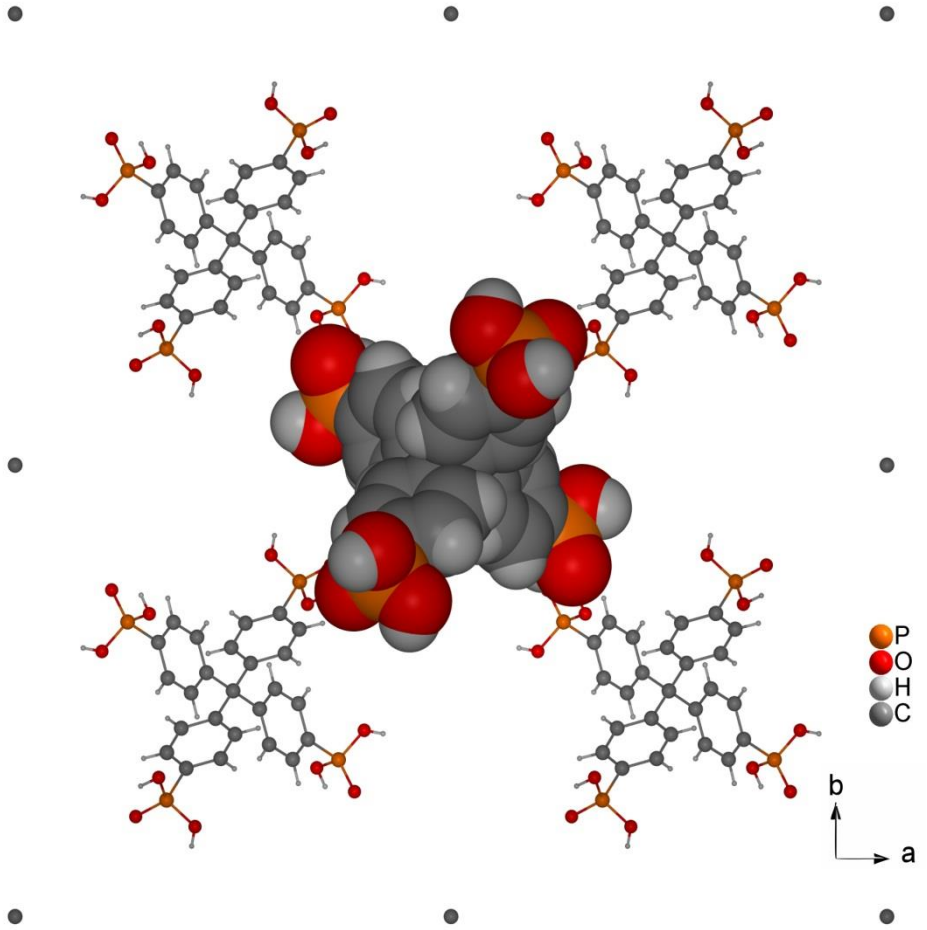

Figure S15. A tetragonal arrangement of 4PE-held linear columns in adduct **3** crystal. Grey isolated atoms are quaternary carbon ones from TPPM molecules.

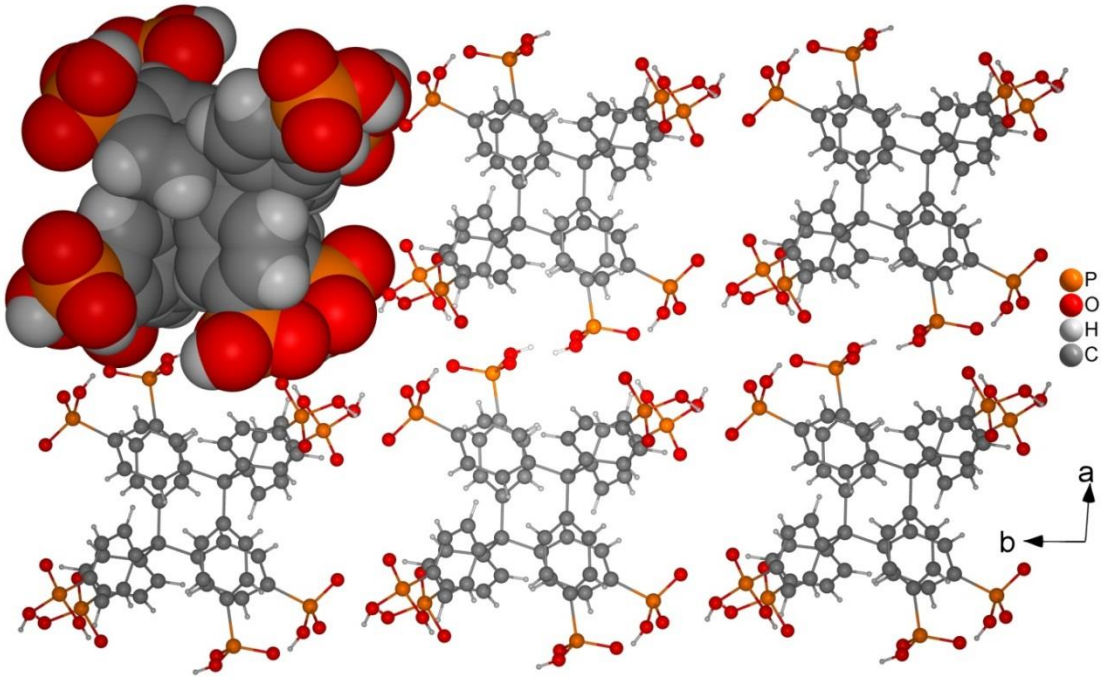

Figure S16. Dimeric assembly of TPPM molecules in adduct **5** presenting 6PE interaction, showed along the [001] direction. These TPPM molecules showed using a space-filling model with arbitrarily chosen atomic radii. The other ones are ball-and-stick representations.

Discussion of 2D Fingerprint plot properties of the cocrystal and acid-base adduct

In our previous work,[3] we demonstrated and discussed specific properties of Hirshfeld surfaces and fingerprint plots of phosphonic acids, in which a phosphonic group is protonated and monodeprotonated. It is worth noting that the properties of the Hirshfeld surface of phosphonic cocrystals have not been reported to date. The lack of deprotonation of a TPPM molecule in **3** has an impact on the 2D fingerprint plot. This is illustrated comparatively on structures with 2,2'-bipyridine (**3**) and 4-(N,N-dimethylamino)pyridine (**4**) in Figure S17. Decomposed 2D fingerprint plots are presented in Figure S18.

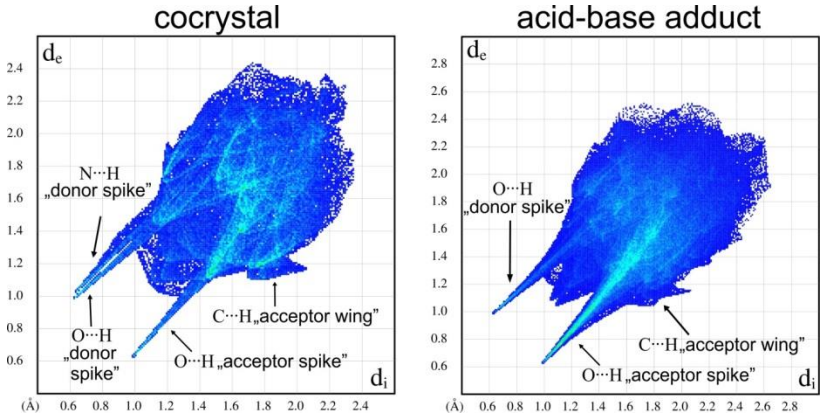

Figure S17. 2D fingerprint plots summarizing contacts of the TPPM molecule in the cocrystal (left) and in the acid-base adduct (right). The 2D fingerprints plots are calculated for structures **3** and **4**, respectively.

O···H and N···H contacts, indicating strong hydrogen bonding, are usually presented in a 2D fingerprint plot as a pair of long sharp spikes directed toward the bottom left of the plot.[4] In the cocrystal structure (**3**), the most prominent feature of the 2D fingerprint plot is the splitting of the upper spike into the N···H and O···H spike. The shortest O···H contacts, expressed as $d_i + d_e$ value, do not differ and in both compounds (**3** and **4**) are within a 1.60-1.62 Å range. The N···H contact is a little more distant (1.64 Å) and this is the reason why it can be distinguished from the O···H spike. In fact, the 2D fingerprint plot of **3** strongly resembles those of free fully-protonated phosphonic acids.[3] This is the case because there are two protonated oxygen atoms per phosphonic group inside the space limited by the Hirshfeld surface of **3**. This increases the contact range and broadens the H···O(N) donor (upper) spike. In structure **4**, where proton transfer occurs, an O···H acceptor (lower) spike dominates. The "wings" found in the 2D fingerprint plot are usually characteristic of C···H interactions. In both instances, a lower wing is present, while the upper one is reduced, indicating the predominance of the C···H accepting character of the tetraphenylmethane core.

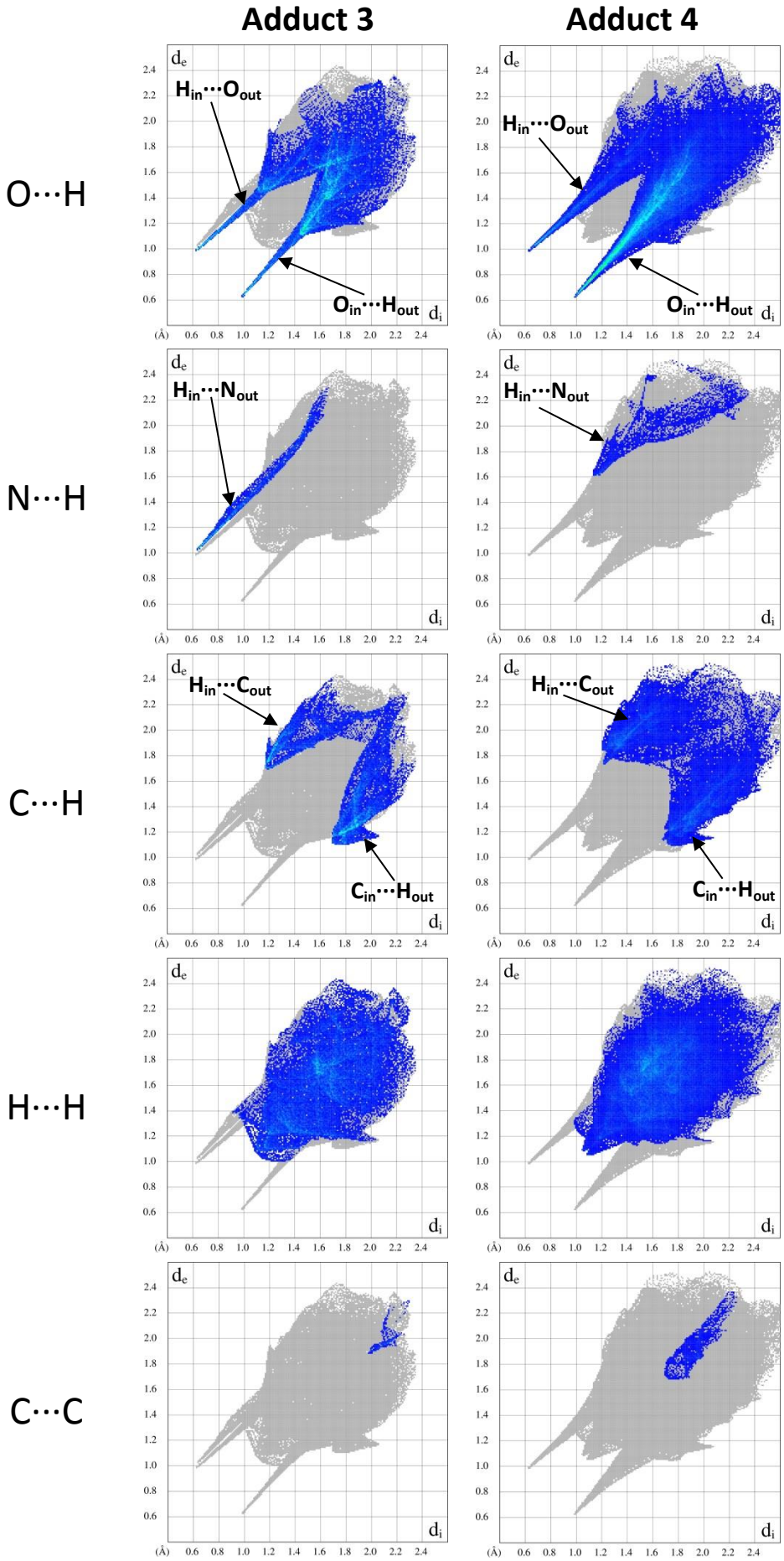

Figure S18. Contact-decomposed 2D fingerprint plots for adducts **3** and **4**.

Discussion of infrared spectra

In the spectrum of acid **1**, in the typical range for hydrogen bonding there are three maxima observed at 3420 cm^{-1}, 2824 cm^{-1}, and 2277 cm^{-1}. A pattern of specific intermolecular interactions present in investigated hydrogen-bonded networks (**2**-**6**) finds its reflection in infrared spectra. The spectral features of adducts **2** and **3** in the range of 3500 – 2000 cm^{-1}, are quite similar to **1** due to the rather noncomplicated hydrogen bond network. There are observable three dominating vibrations (at 3435, 2752, 2286 cm^{-1} and 3430, 2694, 2224 cm^{-1} for **2** and **3**, respectively). This region in adducts **4**-**6** gives much more complex vibrational pattern. For instance in adduct **4** one can find more of strong maxima (3396, 3240, 2924, 2775, 2678, 2342 cm^{-1}) which derive from the hydrogen-bonded networks of water molecules as well as from contribution of protonated bases. This characteristics is the same in adducts **5** and **6** spectra.

The spectrum of tetraphosphonic acid **1** constitutes the basis for an analysis of infrared spectra of adducts **2**-**6**. Most characteristic features, present in all spectra, are: C-C stretching vibrations within phenyl rings (around 1600 cm^{-1} and 1400 cm^{-1}), C-P stretching (750 - 740 cm^{-1}) and the "umbrella" bending of a PO_3 group that occurs at 550-560 cm^{-1}. In **1**, one can notice P=O stretching vibration (1207 cm^{-1}) typical for the protonated phosphonic group as well as asymmetric and symmetric P-$(OH)_2$ stretching at 1017 and 939 cm^{-1}, respectively.

Infrared spectra of adducts (**2**-**6**) give more complicated pattern in the region below 1500 cm^{-1} due to overlapping with signals from base molecules, as well as due to nonuniform deprotonation of phosphonic groups. Additionally, the involvement of the phosphonic groups into the hydrogen bond network may result in coupling of vibrations giving further complication of the spectra.[5] Therefore, assignments should be treated tentatively, especially between 1300 cm^{-1} and 800 cm^{-1}. In the adducts spectra, a monodeprotonated phosphonic group gives usually asymmetric and symmetric PO_2 stretching vibrations centered at 1140 and 1040 cm^{-1}, respectively. The stretching vibration involving a protonated oxygen atom (P-OH) is found at around 930 cm^{-1}.

In adduct **2**, a pyridine molecule introduces C-C pyridine ring stretching vibration at 1634 cm^{-1} and C_{Ar}-N stretching vibration at 1551 cm^{-1}. In this region, contribution from symmetric bending C_{Ar}-H vibrations at 1487 cm^{-1} can also be noticed. The presence of 2,2'-bipyridine in adduct **3** is manifested by a set of peaks at 1564, 1472, 1429 coming from C_{Ar}-N and C-C vibrations in aromatic rings. In this adduct, the presence of not deprotonated phosphonic groups results in the well defined P=O stretching vibration (1215 cm^{-1}) and gives asymmetric and symmetric P-$(OH)_2$ stretching at 989 and 936 cm^{-1}, respectively.

Vibrations of the DMAP molecule in adduct **4** are highly characteristic what has been shown in our previous report.[3] The 1648 cm^{-1} band is assigned to C-C pyridine ring stretching vibrations and maximum at 1560 cm^{-1} is attributed the C_{Ar}-N stretching vibration. Their high intensity causes relative decrease in the intensity of vibrations coming from C-C stretching of the phenyl rings in the tetraphenylmethane core (1399 cm^{-1}). Moreover, there is also found a band centered at 1220 cm^{-1}, that can be attributed to ν_{as}(N-$(CH_3)_2$) vibration.

In the spectrum of adduct **5**, C-N streching bands of 1,6-hexanediamine are centered at 1252 cm^{-1}, 1237 cm^{-1}, and 1017 cm^{-1}. The -NH_3^+ bending vibrations appear as a broadened band at 1526 cm^{-1}. Bands in the range of 1350 cm^{-1} – 1500 cm^{-1} are found due to different vibration deformation modes of CH_2 groups in a hexane chain.

The presence of urotropine, DMSO molecules and lattice water leads to a very complicated infrared spectrum of **6**. The introduction of the urotropine molecule into the structure provides C-N streching bands at 1261 cm^{-1} and 1016 cm^{-1}. Bending vibration modes of methylene groups are positioned at 1368 cm^{-1} and 1465 cm^{-1}, respectively. DMSO gives a set of noticeable signals. The 1076 cm^{-1} band can be ascribed as S=O stretching vibration. The peaks at 1437 cm^{-1} and 1403 cm^{-1} correspond to asymmetric bending mode of the CH_3 group, while a band at 1312 cm^{-1} corresponds to symmetric deformation of the methyl group.

pH-potentiometry studies

Experimental

The potentiometric studies were carried out using a MOLSPIN 1000 automatic titration system at constant temperature of 25 °C, under nitrogen flow. The titration system was equipped with a Mettler Tolledo InLab Micro Pro microcombined electrode calibrated daily in hydrogen ion concentration using HNO_3. Titrations were performed on solutions of 0.1 $mol \cdot dm^{-3}$ KNO_3 as background electrolyte, and the ionic product of water for these conditions was $10^{-13,77}$ $mol^2 \cdot dm^{-6}$. Initial solutions of TPPM were titrated with sodium hydroxide (C = 0.098642 $mol \cdot dm^{-3}$) delivered by 0.25 cm^3 micrometer Hamilton syringe in pH range 2-11. Sample volumes were 2 cm^3, concentration of TPPM was C = 0.00090904 $mol \cdot dm^{-3}$. Stability constants $\beta_{pqr}=[M_pH_qL_r]/[M]^p[H]^q[L]^r$ were calculated using the SuperQuad v. 5.20 program.[6]

Discussion

The TPPM molecule has eight potential protonation sites derived from four phosphonic groups, but in our titration conditions only five protonation constants were found. The rest of the protonation constants are too low ($pK_a < 2$) to be determined in experimental conditions, and also due to precipitation of the compound at low pHs. The values of the protonation constants are presented in Table S3, while Figure S19 shows the graphic representation of the calculated protonation scheme. TPPM (below denoted as H_8L) is totally deprotonated at a pH above 11 and the first four protons are easily deprotonated.

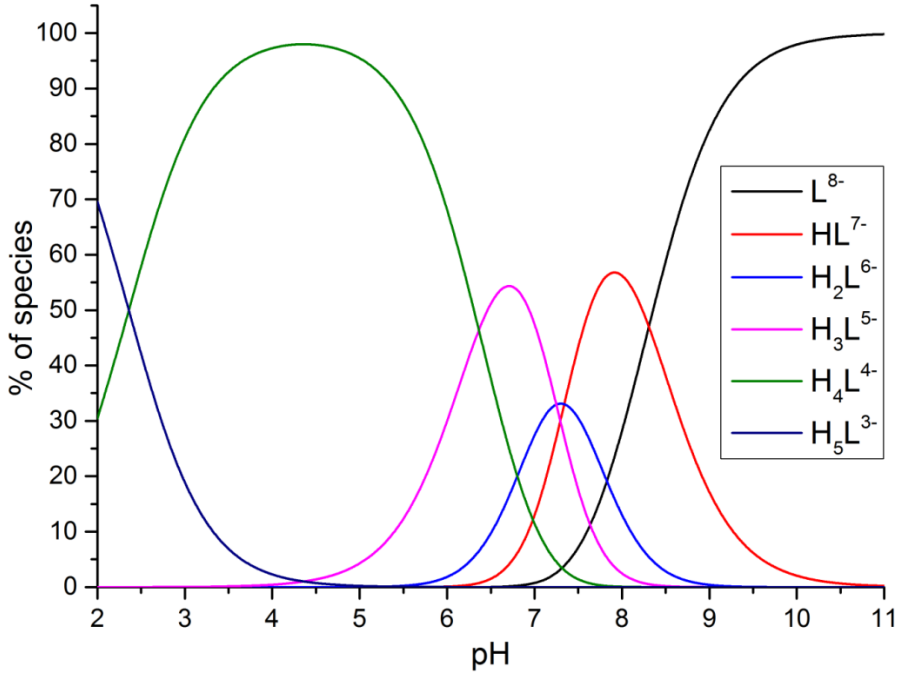

Figure S19. Distribution of protonation forms of L at 25 °C, I = 0.1 $mol \cdot dm^{-3}$ KNO_3

Table S1. Protonation Constants of H_8L at 25 °C and I = 0.1 mol·dm^{-3} (KNO_3)

Equilibrium	logβ	logK_a
$H^+ + L^{8-} = HL^{7-}$	8.31(1)	8.31
$H^+ + HL^{7-} = H_2L^{6-}$	15.66(1)	7.35
$H^+ + H_2L^{6-} = H_3L^{5-}$	22.90(1)	7.24
$H^+ + H_3L^{5-} = H_4L^{4-}$	29.26(1)	6.36
$H^+ + H_4L^{4-} = H_5L^{3-}$	31.62(2)	2.36

The protonation constants for tetraphosphonic acids remain largely unreported in the literature. The compound we examined has four phenyl rings connected into the quaternary carbon atom, and the phosphonic groups are in *para* positions. According to Nagarajan *et al.*, a simple phenylphosphonic acid has two protonation constants pK_1 = 1.80 and pK_2 = 7.50[7], while Guliński *et al.* found the values of pK to be slightly higher (pK_1 = 2.11 and pK_2 = 8.15)[8].

The values of second protonation constants for every phosphonic group present in TPPM are in good agreement with the corresponding constants for phenylphosphonic acid. Generally, acids containing more than two phosphonic groups represent an increase in the basicity of the unprotonated anion.[9] In accordance with these results, the value of pK_1 = 8.31 is slightly higher than for the simple phenylphosphonic acid.

The other acid somehow comparable to TPPM is 1,3,5-benzenetri(phosphonic acid) with three phosphonic groups connected to the aromatic ring. Five protonation constants were found for this compound.[10] The values of the protonation constants are higher than for aromatic diphosphonates[11] but are almost the same as for TPPM. This fact confirms that the higher the presence of phosphonic groups in the acid, the higher the amount of protonation constants.[9]

References

(1) Ng, M. C. C.; Craig, D. J.; Harper, J. B.; van-Eijck, L.; Stride, J. A., The Central Atom Size Effect on the Structure of Group 14 Tetratolyls. *Chemistry – A European Journal* **2009,** 15, (27), 6569-6572.

(2) Yang, G.; Shen, C.; Zhang, L.; Zhang, W., Nickel-catalyzed Arbuzov reactions of aryl triflates with triethyl phosphite. *Tetrahedron Lett.* **2011,** 52, (39), 5032-5035.

(3) Białek, M. J.; Zaręba, J. K.; Janczak, J.; Zoń, J., Chains, layers, channels, and more: Supramolecular chemistry of potent diphosphonic tectons with tuned flexibility. the generation of pseudopolymorphs, polymorphs, and adducts. *Cryst. Growth Des.* **2013,** 13, (9), 4039-4050.

(4) McKinnon, J. J.; Spackman, M. A.; Mitchell, A. S., Novel tools for visualizing and exploring intermolecular interactions in molecular crystals. *Acta Crystallogr. Sect. B: Struct. Sci.* **2004,** 60, (6), 627-668.

(5) Zoń, J.; Videnova-Adrabinska, V.; Janczak, J.; Wilk, M.; Samoć, A.; Gancarz, R.; Samoć, M., Design, synthesis and noncentrosymmetric solid state organization of three novel pyridylphosphonic acids. *CrystEngComm* **2011,** 13, (10), 3474-3484.

(6) Gans, P.; Sabatini, A.; Vacca, A., SUPERQUAD: an improved general program for computation of formation constants from potentiometric data. *J. Chem. Soc., Dalton Trans.* **1985**, (6), 1195-1200.

(7) Nagarajan, K.; Shelly, K. P.; Perkins, R. R.; Stewart, R., Arylphosphonic acids. I. Substituent effects on their first and second dissociations. *Can. J. Chem.* **1987,** 65, (8), 1729-1733.

(8) Gulinski, J.; Maciejewska, U.; Stewart, R., The effects of high concentrations of aqueous tetramethylammonium chloride and other salts on the dissociation of phenylphosphonic acid and on the enolization of acetone. *J. Solution Chem.* **1988,** 17, (4), 297-304.

(9) Bogdan, C.; Peczely, G.; Gaizer, F., Protonation constants of ethane and propane frame-substituted oligophosphonic and oligophosphonocarboxylic acids. *Polyhedron* **2001,** 20, (15-16), 1809-1813.

(10) Kong, D.; Clearfield, A.; Zoń, J., Crystal-engineered three-dimensional hydrogen-bonding networks built with 1,3,5-benzenetri(phosphonic acid) and bipyridine synthons. *Cryst. Growth Des.* **2005,** 5, (5), 1767-1773.
(11) Caplan, N. A.; Pogson, C. I.; Hayes, D. J.; Blackburn, G. M., Novel bisphosphonate inhibitors of phosphoglycerate kinase. *Bioorg. Med. Chem. Lett.* **1998,** 8, (5), 515-520.